RSC Advances

ROYAL SOCIETY
OF CHEMISTRY

www.rsc.org/advances

Journal Name

COMMUNICATION

SWCNT/BiVO$_4$ Composites as Anode Materials for Supercapacitor Application

Ziyauddin Khan,[a] Shateesh Bhattu[b] Santosh Haram[b] and Deepa Khushalani[a]*

In this report, we have systematically investigated the effect of SWCNTs on the electrochemical performance of BiVO$_4$: a material not studied for energy storage. Loading of 20 wt% SWCNTs with BiVO$_4$ exhibited highest specific capacitance (395 F g^{-1}) and up to 88% coloumbic efficiency was obtained over 200 cycles of charge/discharge for this composite.

Supercapacitors, commonly known as electrochemical capacitors (ECs), are unique energy storage devices due to their high power density compared to secondary batteries and they also have a high energy density when compared to conventional electrostatic capacitors.[1,2] ECs, depending on charge storage mechanism, can be classified into two main categories namely, electrical double layer capacitors (EDLC) and pseudocapacitors. The latter derives its energy from fast and reversible faradic reactions that occur at the electrode/electrolyte interface. Since such fast redox reactions usually take place in materials where metal ions have multiple oxidation states, therefore, transition metal oxides are of great importance for pseudocapacitors.[3] RuO$_2$, MnO$_2$, NiO, Co$_3$O$_4$, V$_2$O$_5$ and Ni(OH)$_2$ materials have been investigated for pseudocapacitor based applications as cathode materials in order to enhance the power and energy densities.[4-7] Moreover, predominantly in these cases, activated carbon (AC) has been used as the anode material which normally does not contribute substantially to the overall energy density.[8] It has been purported that energy density of the supercapacitors can be improved by replacing the traditional AC with oxides materials which can work as the anode. So far there have been few reports on formation of new anode materials.[8-11]

Presented here is the use of Bismuth Vanadate (BiVO$_4$), a novel anode material for supercapacitor based applications. This is an attractive transition metal oxide because of its unique properties and thus far it has predominantly been evaluated for gas sensing, ferroelasticity and most recently for photocatalytic activity. It is known, however, to suffer from low electronic conductivity.[12] A valuable strategy for improving electronic conductivity has been to form a composite with a conductive agent. It should be noted that thus far, predominantly various porous and conductive carbon materials having high a surface area such as activated carbons, graphene oxide, graphene and carbon nanotubes (CNTs) have been widely studied to form a composite with the metal oxide for energy storage based devices.[13,14] SWCNTs (Single walled carbon nanotubes) are found to be an attractive material which can improve the electronic conductivity predominantly in combination with electroactive materials because of their excellent conductivity, low density and good mechanical and chemical stability.[15] Therefore, herein, we investigated the effect of SWCNTs on the electrochemical performance of BiVO$_4$. The electrochemical properties of pure and SWCNT/BiVO$_4$ composite were examined by using cyclic voltammetry (CV) and galvanostatic charge-discharge (CD) technique in presence of exclusively Na$^+$ ion containing aqueous electrolyte.

BiVO$_4$ was synthesised by solvothermal route and loading of SWCNT was done by simple ultrasonicaton method (see *Supplementary Information* for details). We have systematically studied the effect of 5, 10, 20, 25, 50 and 75 wt% loading of SWCNTs on the electrochemical performance of BiVO$_4$ however, data will only be presented for 10, 20 and 25 wt% loadings (see *SI* for data on the rest of the samples). 10, 20 and 25 wt% SWCNT/BiVO$_4$ composite have been termed as S1, S2 and S3. For electrochemical characterization, Pt as counter electrode and Hg/HgO as reference electrode was used with 2M NaOH electrolyte in all experiments.

The purity and crystallinity of the solvothermally synthesized BiVO$_4$ was analysed by powder X-ray diffraction, Fig. 1. It is clear that the product crystallized well and the diffractogram fitted perfectly to a monoclinic scheelite structure and the peaks could be indexed according to reported data (JCPDS No. 75-2480). From FE-SEM images it can be observed that BiVO$_4$ consisted of 15-20 nm sized spherical particles that agglomerated and formed larger porous oval shaped structures with sizes in the range of 200-300 nm (inset Fig. 1). The energy-dispersive X-ray (EDX) pattern for BiVO$_4$ confirmed the presence of Bi, V and O elements (Fig S1a and b, *SI*). The quantitative analysis revealed the atomic ratio of

Bi^{3+}: V^{5+} as 1:1, thereby confirming the stoichiometry. BET surface area of $BiVO_4$ was measured by N_2 adsorption–desorption isotherm (Fig. S2, *SI*). The N_2 sorption measurement displayed a typical type III isotherm and BET surface area was found to be 15 m^2 g^{-1}. This value is 10 times higher than the reported value for $BiVO_4$ thus far.[16]
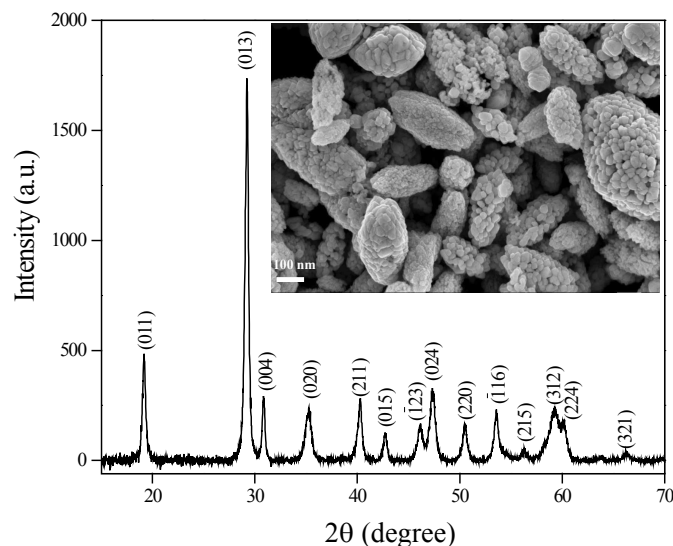
Fig. 1 Powder X-ray diffraction pattern and inset shows FE-SEM image of solvothermally synthesised $BiVO_4$

The electrochemical behaviour of pure $BiVO_4$ was evaluated by CV under various scan rates ranging from 5 to 100 mV s^{-1} (Fig 2a). The redox peaks observed were assigned to the reversible faradic processes of Bi [Bi (III) ↔ Bi] *via* electrolytic ion diffusion.[17] A single peak with high current was detected for reduction (-0.8 V) while for oxidation, two peaks were observed (-0.57 V and -0.42 V). The single reduction peak was attributed to the reduction of Bi (III) to Bi metal whereas the two oxidation peaks were due to the oxidation of Bi metal to Bi (III). The oxidation peak A1 has been purported to the oxidation of metallic Bi to Bi^+ due to the formation of Bi metal layer at Bi-metal/solution interface.[18] The redox peaks were found to be reproducible at higher scan rates, however, the reduction and oxidation peaks were shifted upon increasing scan rate assigned to the internal resistance drop.[19] An increase in the current response with higher scan rate clearly indicated that the kinetics of interfacial faradic redox reactions and the rates of electronic and ionic transport were rapid enough as they were easily observed at high scan rates. This suggests that $BiVO_4$ could be a good anode material for aqueous supercapacitors.
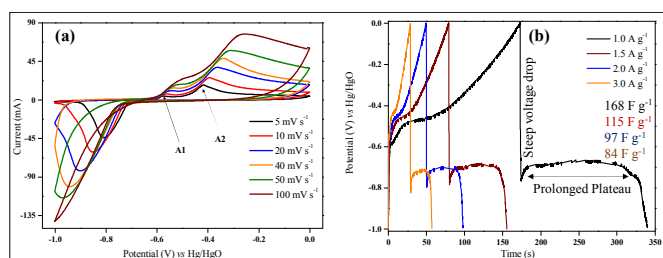
Fig. 2 (a) CV and (b) charge-discharge profile of $BiVO_4$ at various scan rates

The electrochemical capacitance of $BiVO_4$ was evaluated by galvanostatic CD. The CD curves (Fig. 2b), at different current densities ranging from 1 to 3 A g^{-1} between voltage window -1.0 and 0.0 V appeared to be non-symmetric with an associated IR drop.

This behaviour is different from typical EDLC which insinuates pseudocapacitive nature of $BiVO_4$. Despite steep voltage drop (upon the first few seconds of discharge) which is ascribed to internal resistance, we observed strikingly prolonged plateau of voltage output due to the involvement of faradaic process in $BiVO_4$. The calculated specific capacitances were 168, 115, 97, and 84 F g^{-1} at current densities of 1.0, 1.5, 2.0 and 3 A g^{-1}, respectively. It was also detected that with increasing current densities, the specific capacitance decreased gradually, which can be attributed to the diffusion of electrolytic ions into the electroactive materials at low current densities. At higher current densities, diffusion effect limits the migration of the electrolytic ions, thereby this caused some of the active surface of the material to become inaccessible for charge storage.[20] Good cycling stability is another significant feature for high-performance supercapacitors. The cyclic performance of $BiVO_4$ is displayed in Fig. S3, *SI* at 1 A g^{-1} current density for 200 cycles. It was observed that the discharge capacity retained only 42 % up to 200 cycles. Unexpectedly, $BiVO_4$ displayed enormous (38 %) drop in specific capacitance within first 10 cycles. This huge drop in capacitance may be due to the low electronic conductivity of $BiVO_4$. Therefore, in order to improve its electrochemical activity, SWCNTs (at varying ratios) were combined with $BiVO_4$ *via* ultrasonication.

It was determined through powder X-ray diffraction that the prepared S1, S2 and S3 composites clearly showed well-resolved peaks due to presence of $BiVO_4$ and there were no deleterious effects observed due to the ultrasonication procedure (Fig. S4, *SI*). This was valid whether SWCNTs were incorporated or not. In addition, SEM images of the composite clearly showed the separate two phases of $BiVO_4$ and the SWCNT (Fig. S5, *SI*). N_2 adsorption desorption isotherm was performed to evaluate surface area of S1, S2 and S3 samples and it was observed that all adsorption desorption isotherms followed type III isotherm (Fig. S6, *SI*). The BET surface areas for S1, S2 and S3 increased gradually with increased loading level of SWCNTs and values of 35 m^2 g^{-1}, 53 m^2 g^{-1} and 56 m^2 g^{-1} were obtained for the three samples respectively.

The electrochemical performances of S1, S2 and S3 were also evaluated by CV and CD technique at various scan rates. It was observed that the CV profiles for these three composites were similar to the $BiVO_4$ profile indicating that SWCNTs did not affect $BiVO_4$ chemically and the observed redox peaks were due to faradic processes (Fig S7, *SI*) of $BiVO_4$.

Current Density (A g^{-1})	Specific Capacitance (F G^{-1})		
	S1	S2	S3
2.50	350	395	224
3.75	273	315	163
5.0	247	291	147
7.5	232	272	121
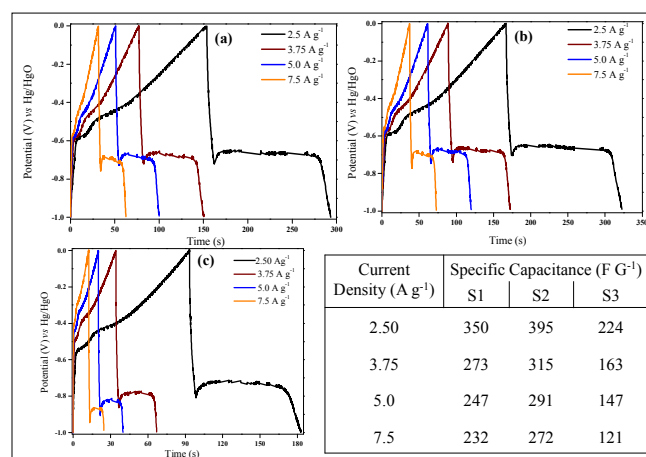
Fig. 3 (a), (b) & (c) charge-discharge profile and table shows specific capacitance at of S1, S2 and S3 at different current densities.

The charge–discharge curves of S1, S2 and S3 (Fig. 3) at different current densities in voltage window -1.0 and 0.0 V display nonlinearities, different from typical EDLC behaviour and similar to

Journal Name | COMMUNICATION

CD profile of BiVO$_4$ (Fig. 2b) which indicated the pseudocapacitive nature of materials for charge storage application. Similar CD profile of S1, S2 and S3 *w.r.t.* BiVO$_4$ confirms that SWCNTs were not playing any role in the faradic process. The specific capacitance was found to be 350 F g^{-1} for S1 at 2.5 A g^{-1} which improved with increased loading level of SWCNTs (for S2 395 F g^{-1} at 2.5 A g^{-1}). Note that mass loadings of the electrode have been provided in Table S1, *SI*. The high conductive nature of SWCNT leads to good electron transport, thereby improving the specific capacitance of composites. However, further enhancement in loading level of SWCNTs caused a drop in specific capacitance (for S3 224 F g^{-1} at 2.5 A g^{-1}). Thus, it was observed that S2 gave the highest specific capacitance at 2.5 A g^{-1} current density compared to BiVO$_4$, S1 and S3. This could be attributed to improved surface area and enhanced electronic conductivity due to the presence of SWCNTs. However, the decrease in specific capacitance for S3 may be ascribed to the inaccessibility of redox sites of BiVO$_4$ due to high concentration of SWCNTs. Hence, the optimized the loading level of SWCNTs with BiVO$_4$ was found at 20 wt%. Upon increasing the current density, the specific capacitance for S2 decreased gradually from 395 F g^{-1} to 272 F g^{-1}. This can be ascribed to the diffusion effect of electrolytic ions. It was analogously observed that the For complete data set for all samples synthesized, refer to Table S2, *SI*.

Fig. 4 displays the cycle performance of BiVO$_4$, S1 and S2 measured at current density 1.0 A g^{-1}, 2.5 A g^{-1} and 2.5 A g^{-1}, respectively for 200 cycles. From Fig. 4, noticeably, 42% and 58% capacitance was retained for BiVO$_4$ and S1. However, it was observed that the stability of material was improved dramatically by increasing the loading amount of SWCNT up to 20 wt% and 88% of capacitance was retained up to 200 cycles at current density of 2.5 A g^{-1} (compare to BiVO$_4$) which showed the high rate capability and excellent long-term stability of S2. As discussed in galvanostatic CD section for BiVO$_4$, we noted 38% of specific capacitance dropped within first 10 cycles, however, for S2 no such large drop in specific capacitance was detected. This unique behaviour can be ascribed to improved electronic conductivity by the addition of SWCNTs. Subsequently, the coulombic efficiency was also found to be 84% retained at high current density 2.5 A g^{-1}, indicating excellent long-term stability of S2 sample (Fig. S8, *ESI*).
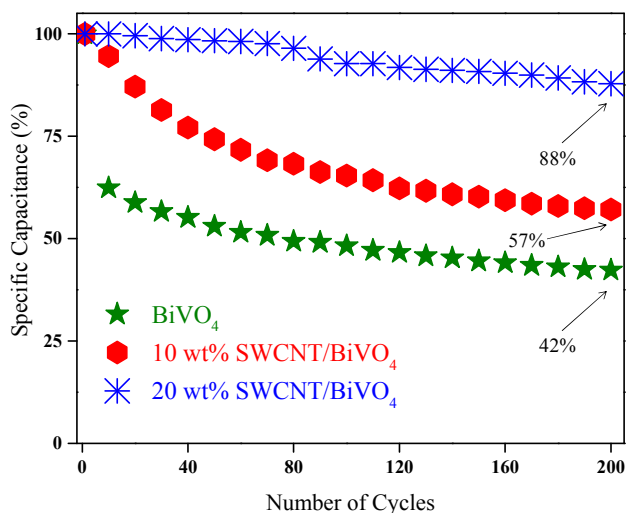
Fig. 4 Cyclic performance in terms of specific capacitance (%) of BiVO$_4$, S1 and S2 at current density of 1.0 A g^{-1}, 2.5 A g^{-1} and 2.5 A g^{-1}, respectively

In conclusion, BiVO$_4$ and SWCNT/BiVO$_4$ composites have been synthesized and their electrochemical performance was evaluated by CV and galvanostatic charge-discharge measurements in 2M NaOH electrolytic solution. It was observed that 20 wt% SWCNT/BiVO$_4$ composite was the optimized anode material when compared to the others in terms of specific capacitance, cyclic stability and coulombic efficiency. It is believed, that this study provides a new direction to explore SWCNT/BiVO$_4$ based anode materials for aqueous supercapacitors with high capacitance.

Notes and references

^{a}Materials Chemistry Group, Department of Chemical Sciences, Tata Institute of Fundamental Research, Mumbai 400005, India.
Email: khushalani@tifr.res.in
^{b}Department of Chemistry, University of Pune, Pune 411007, India.

1   P. Simon and Y. Gogotsi, *Nat. Mater.*, 2008, **7**, 845.
2   A. S. Arico, P. Bruce, B. Scrosati, J. M. Tarascon and W. V. Schalkwijk, *Nat. Mater.*, 2005, **4**, 366.
3   Q. Lu, J. G. Chen and J. Q. Xiao, *Angew. Chem. Int. Ed.*, 2013, **52**, 1882.
4   H. Kim and B. N. Popov, *J. Power Sources*, 2002, **104**, 52.
5   Z. S. Wu, W. C. Ren, D. W. Wang, F. Li, B. L. Liu and H. M. Cheng, *ACS Nano*, 2010, **4**, 5835.
6   J.-W. Lang, L.-B. Kong, W.-J. Wu, Y.-C. Luo and L. Kang, *Chem. Commun.*, 2008, **44**, 4213.
7   H. L. Wang, H. S. Casalongue, Y. Y. Liang and H. J. Dai, *J. Am. Chem. Soc.*, 2010, **132**, 7472.
8   W. Tang, L. Liu, S. Tian, L. Li, Y. Yue, Y. P. Wu and K. Zhu, *Chem. Commun.*, 2011, **47**, 10058.
9   J. B. Jiang, J. L. Liu, S. J. Peng, D. Qian, D. M. Luo, Q. F. Wang, Z. W. Tian and Y. C. Liu, *J. Mater. Chem. A*, 2013, **1**, 2588.
10 Q. T. Qu, Y. S. Zhu, X. W. Gao and Y. P. Wu, *Adv. Energy Mater.*, 2012, **2**, 950.
11 D. Choi, G. E. Blomgren and P. N. Kumta, *Adv. Mater.*, 2006, **16**, 1178.
12 Y. Park, K. J. McDonald and K.-S. Choi, *Chem. Soc. Rev.*, 2013, **42**, 2321.
13 L.-Y. Lin, M.-H. Yeh, J.-T. Tsai, Y.-H. Huang, C.-L. Sun, K.-C. Ho, *J. Mater. Chem. A*, 2013, **1**, 11237.
14 S.-D. Xu, Y.-B. Zhu, Q.-C. Zhuang and C. Wu, *Mater. Res. Bull.*, 2013, **48**, 3479.
15 M. Sathiya, A. S. Prakash, K. Ramesha, J-M. Tarascon and A. K. Shukla, *J. Am. Chem. Soc.*, 2011, **133**, 16291.
16 M-L. Guan, D-K. Ma, S-W. Hu, Y-J. Chen and S-M. Huang, *Inorg. Chem.*, 2011, **50**, 800.
17 B. Sarma, A. L. Jurovitzki, Y. R. Smith, S. K. Mohanty and M. Misra, *ACS Appl. Mater. Interfaces*, 2013, **5**, 1688.
18 V. Vivier, A. Regis, G. Sagon, J.-Y. Nedelec, L. T. Yu and C. Cachet-Vivier, *Electrochimica Acta*, 2001, **46**, 907.
19 L-Q. Mai, F. Yang, Y-L. Zhao, X. Xu, L. Xu and Y.-Z. Luo, *Nat. Commun.*, 2011, **2**, 381.
20 J. Yan, Z. Fan, W. Sun, G. Ning, T. Wei, Q. Zhang, R. Zhang, L. Zhi and F. Wei, *Adv. Funct. Mater.*, 2012, **22**, 2632.

RSC Advances Accepted Manuscript